ChemSusChem

Research Article
doi.org/10.1002/cssc.202300535

Chemistry Europe
European Chemical Societies Publishing

www.chemsuschem.org

On the Rich Chemistry of Pseudo-Protic Ionic Liquid Electrolytes

Luke Wylie,[a] Mónika Kéri,[b] Antal Udvardy,[b] Oldamur Hollóczki,[b] and Barbara Kirchner*[a]

Mixing weak acids and bases can produce highly complicated binary mixtures, called pseudo-protic ionic liquids, in which a complex network of effects determines the physicochemical properties that are currently impossible to predict. In this joint computational-experimental study, we investigated 1-methylimidazole-acetic acid mixtures through the whole concentration range. Effects of the varying ionization and excess of either components on the properties, such as density, diffusion coefficients, and overall hydrogen bonding structure were uncovered. A special emphasis was put on understanding the multiple factors that govern the conductivity of the system. In the presence of an excess of acetic acid, the 1-methylimidazolium acetate ion pairs dissociate more efficiently, resulting in a higher concentration of independently moving, conducting ions. However, the conductivity measurements showed that higher concentrations of acetic acid improve the conductivity beyond this effect, suggesting in addition to standard dilution effects the occurrence of Grotthuss diffusion in high acid-to-base ratios. The results here will potentially help designing novel electrolytes and proton conducting systems, which can be exploited in a variety of applications.

Introduction

The theory of acid-base equilibria is among the most fundamental concepts in modern chemistry.[1,2] While predicting the chemistry of weak bases and acids in dilute aqueous solutions is a routine exercise, describing their behavior in concentrated mixtures with each other is still highly challenging, due to the complexity of the underlying physical chemical effects.[3,4] Such compounds are often referred to as pseudo-ionic liquids,[5,6] highlighting their chemical similarity to ionic liquids (ILs), while also showcasing that their ionization is incomplete. Since it is possible to exploit the mobility of protons in a number of modern applications,[7] including electrolytes in energy devices,[8] these systems are interesting beyond the mere academic point of view, and understanding them is of utmost importance.

The rich chemistry of pseudo-IL translates into conductivity through an elusive web of complicated effects. One of the most important characteristics of these binary materials is the p*K*a difference between the acid and the protonated base, which to some extent determines the degree of ionization, i.e., the concentration of charged species or ionic density, in their mixtures. As a general rule, a $\triangle pKa = 8$ is required for a complete dissociation,[9,10] which can be achieved, for instance, by applying super acids (e.g. HNTf2). The corresponding liquids are termed protic ionic liquids (PILs), which have found a wide range of applications, as described in Refs. [11] and [12]. However, it must be stressed here that p*K*a values are generally available only for dilute aqueous solutions, and since they are susceptible to significant changes upon variation of the medium and the concentration of the components, assessing the degree of ionization is far from trivial. In agreement, Zhu and Forsyth found that these aqueous p*K*a data show no direct relation to the mobility of protons in the solution.[13]

After some of the species in the system undergo ionization through (partial) proton transfer from the acid to the base, conductivity requires that the anion and cation move independently in the solution. On one hand, this means that the ions need to be mobile, in which a low viscosity is a clear advantage. The mobility can be increased by adding molecular solvents (e.g., water, DMSO) to the given species, which – despite decreasing the ionic density of the system – decreases viscosity, resulting in higher mobility and conductivity.[14,15] On the other hand, the formation of ion pairs, as it has been discussed in the literature of ionic liquids extensively,[16–18] results in a correlation of the motion of these oppositely charged species, and therefore their diffusion does not result in an effective transport of charge. In this regard, the role of the medium is again emphasized, as it can be a determining factor in triggering or hindering ion pairing.

It has also been evidenced in literature that through the numerous kinds of interactions between anions and cations of ILs, charge can be transferred between these species, decreasing the effective charge of the ions to a fraction of ± 1.[18,19] This reduction of charge decreases the charge transport within the liquid, which results in a lowered conductivity. In case of

[a] Dr. L. Wylie, Prof. Dr. B. Kirchner
University of Bonn, Clausius Institute of Physical and Theoretical Chemistry, Mulliken Center for Theoretical Chemistry, Beringstr. 4, 53115 Bonn, Germany
E-mail: kirchner@thch.uni-bonn.de

[b] Dr. M. Kéri, Dr. A. Udvardy, Prof. Dr. O. Hollóczki
University of Debrecen, Department of Physical Chemistry, Egyetem tér 1, 4032 Debrecen, Hungary

Supporting information for this article is available on the WWW under https://doi.org/10.1002/cssc.202300535

(aprotic) ILs, correcting for these effects in the Nernst–Einstein formula enabled obtaining a closer connection between the ion mobilities and conductivities, indicating that the low ionicities measured for these liquids can be, at least partially, related to this charge transfer.[19]

Finally, the conductivity can be enhanced by structural (or Grotthuss) diffusion,[20] in which the rearrangement of covalent and weaker secondary interactions (e.g. hydrogen bonds) in a network of interplay within the liquid enables the facile transfer of charge through space without any actual long-range spatial movement of atoms. Thus, ion mobility becomes irrelevant after a fashion, since the charge transfer can bypass sluggish diffusion. The most well-known example of this behavior is the proton and hydroxide conductivity in aqueous solutions. In ILs unusual, anionic Grotthuss diffusion mechanisms have also been reported.[21–24] For efficient Grotthuss diffusion, there are several pre-requisites that need to be considered. First, the aforementioned extensive network of secondary interactions is necessary, which provides the foundation for the covalent rearrangement described above. This, furthermore, requires the presence of amphoteric species in the system (e.g. water molecules) that are capable of building these networks, and accepting/releasing the mobile species, most often a proton. Finally, the rearrangement of the covalent and secondary bonds needs to occur through a low barrier, which allows for the fast transfer of charge between the molecules that constitute the network of interactions.

In a system that undergoes Grotthuss diffusion, the mobility of the proton can be discussed on three separate time scales.[25] The first one is proton rattling, which is the back and forth transfer of the proton between an acid-base pair. While it is possible to observe, it does not contribute to the effective conductivity of the system. The second is the lifetime of the stable charge, which is determined by the hopping of protons through the hydrogen bonding network, inducing the extra conductivity arising from the Grotthuss diffusion. This is facilitated by low barriers for the proton transport, for which values around 2 kcal mol^{-1} are reported in literature for highly conductive systems.[25,26] The third, longest time scale process is the reorientation of ions, in which the mobile proton is taken out of a hydrogen bond channel through the translation and/or rotation of the ions, and then released elsewhere.

From the literature, a picture emerges that in "pure" PILs Grotthuss diffusion is not possible.[25,27] The reason for this general wisdom might in part lie in the fact that amphoteric cationic and anionic species that would participate in a hydrogen bonding network capable of shuttling the mobile protons are seldom available. However, Zhu and Forsyth observed for the amphoteric H_2PO^- ion in combination with 1-methylimidazole, and observed no Grotthuss mechanism assisting the conductivity.[13] These results indicate that structural diffusion in fully ionic substances may be hindered by further, hitherto unconsidered effects as well. Through mixing ILs with amphoteric compounds – such as water, imidazole, or carboxylic acids – channels of hydrogen bonds can be formed, allowing structural diffusion. This may trigger an increase in conductivity beyond the direct effects of ion diffusion.[25,28] However, it must be kept in mind that by introducing these species, some of the attractive properties that ILs often possess, such as inertness and low vapor pressure, may be lost.[29] In this regard, pseudo-PILs are of particular interest, since they inherently contain the neutral base and acid, which may serve as amphoteric molecules necessary for inducing enhanced conductivity. However, it is not yet clear how the delicate balance between these complex effects influences the conductivity of these promising materials, which hampers their extensive application.

Theoretical chemistry has helped understanding the behavior of PILs,[30] and pseudo-PILs,[31] as well as non-ideal acid-base equilibria.[32] Thus, in this article, a variety of theoretical chemical approaches will be used to shed new light on the conductivity of binary mixtures consisting of weak acids and bases. The chosen compounds will be acetic acid (AA) and 1-methylimidazole (C_1Im)). Due to the methyl group on one of the nitrogen atoms of the C_1Im ring, the base and its conjugate acid cannot participate in the hydrogen bonding network to promote Grotthuss diffusion. This feature simplifies the process in the system, and thereby makes the interpretation of the results somewhat simpler. We employ classical and *ab initio* molecular dynamics (AIMD) simulations, as well as conductivity measurements to observe how the complex network of interactions and physicochemical effects described above contribute to the conductivity of these mixtures.

Initial systems to observe the large-scale change in physical properties of varied ionization using polarizable MD constituted of a four molecule system involving 1-methyl-1-methyimidazolium acetate ([C_1HIm][OAc]) as the ionized compounds and acetic acid (AA) and 1-methylimidazole (C_1Im) as the neutral compounds (see Table 1), with ball-and-stick representations of all compounds together with some labelling shown in Figure 1.

Polarizable MD was completed using a total system size of 500 ion pairs or neutral molecules, with for example for 50:50 systems of ion pair to acetic acid containing 250 [C_1HIm][OAc] ion pairs, 250 C_1Im molecules and 250 AA molecules, with all system compositions studied shown in Table 1. Smaller increments were chosen around the ionization ratios of 20% to 40%. Ionization ratios in this range have been previously shown to

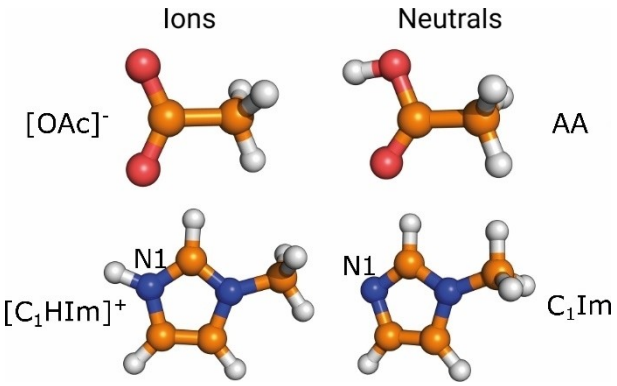

Figure 1. Ball-and-stick representation of compounds applied in this study. Upper left: acetate anion ([OAc]$^-$); upper right: acetic acid (AA); lower left: 1-methyimidazolium cation ([C_1HIm] +); lower right: 1-methylimidazole (C_1Im).

Table 1. Compositions studied at different ionization ratios and thus varying [C1HIm][OAc] to C_1Im or AA added. Ion: Ionization %.

Ion	$[C_1HIm]^+$	$[OAc]^-$	C_1Im	AA
0	0	0	500	500
10	50	50	450	450
20	100	100	400	400
25	125	125	375	375
30	150	150	350	350
35	175	175	325	325
40	200	200	300	300
50	250	250	250	250
100	500	500	0	0

reproduce physical properties, such as conductivity and diffusion coefficients, when comparing experimental and polarizable MD results.[33]

Following this, given prior studies indicating that the theoretical ionization would be around 25:75 ions to neutral molecules,[33] this ratio was used for further analysis of $[C_1HIm][OAc]$ systems with the addition of either neutral C_1Im or AA, see Table 2. Additional neutral C_1Im and acetate were added to be in molar ratios of 25%, 50% and 75% to the 25% ionized $[C_1HIm][OAc]$ IL. These systems were constructed consistently with 500 $[C_1HIm][OAc]$ ion pairs with added C_1Im or AA to reach the final molar ratio. In addition to these IL-neutral mixture systems, control systems containing 1000 C_1Im and AA were also simulated to validate the density and diffusion coefficients of the neat neutral compounds.

AIMD contained the same system composition and definition as the polarizable FF calculations, however, with the total system size scaled down from 500 total ion pairs plus added neutral molecules to a size more manageable for AIMD calculations. These systems constituted of a total of 40/48 ion pairs or neutral molecules added, with neutral molecules added to make up solutions of 50% and 75% neutral molecules added, see Table 2.

Results and Discussion

Effect of ionization ratio variation

Using polarizable MD, the physical properties of [C1HIm][OAc]: AA + C_1Im solutions at various ratios of ionization shown in Table 1 were tested to determine the change of properties with change in the ionization ratio. Within these studies, we aim to extend upon results obtained by Joerg and Schröder,[33] wherein they scanned the full range of ionization ratios with polarizable MD, with our study specifically focusing on the range of 20–40% ionization. It should be noted that as a result of this being polarizable classical MD rather than AIMD, the ionization degree

Table 2. Compositions studied with additional C_1Im or AA in MD and AIMD. MD at constant ionization of 25% ions to neutrals, for AIMD this will be discussed below. MR: Molar Ratio Neutral Component; add: Added Neutral Component. $x_{[C_1HIm]^+C_1Im}$ in last column abbreviated *x*.

MR	add	$[C_1HIm]^+$	$[OAc]^-$	C_1Im	AA	*x*
MD						
100	AA	0	0	0	1000	0
75	AA	125	125	375	1875	0.2
50	AA	125	125	375	875	0.33
25	AA	125	125	375	541	0.43
0	none	125	125	375	375	0.5
25	C_1Im	125	125	541	375	0.57
50	C_1Im	125	125	875	375	0.66
75	C_1Im	125	125	1875	375	0.8
100	C_1Im	0	0	1000	0	1
AIMD						
75	AA	8	8	0	24	0.2
50	AA	16	16	0	16	0.33
50	C_1Im	16	16	16	0	0.66
75	AA	8	8	0	24	0.2

is fixed a priori, with proton transfer being forbidden by the explicit bonding parameters in place between protons and their defined bonding partners. In this analysis, it was found that as the ionization increases with a higher ratio of [C1HIm][OAc] and fewer neutral molecules, the density of the solutions increases. As shown in Figure 2, the pure ionic solution has the highest density at 1.239 g cm^{-3}, whilst the pure neutral compounds have a density of 1.030 g cm^{-3}. This general trend reproduces those found by Joerg and Schröder[33] and thus validate our model for further examination of the specific range of 20–40% ionization.

In terms of replicating the experimental data, the ionization ratio of 50% ionization simulation was found to be the closest to reproducing the experimental value of 1.155 g cm^{-3} proposed by Hou et al.,[34] giving a density of 1.116 g cm^{-3}. In contrast, the 25% ionization sample gave a density of 1.075 g cm^{-3} and thus was found to most effectively reproduce the densities of 1.073 g cm^{-3} and 1.075 g cm^{-3} found in literature by Watanabe et al.[36] and Qian et al.,[35] respectively.

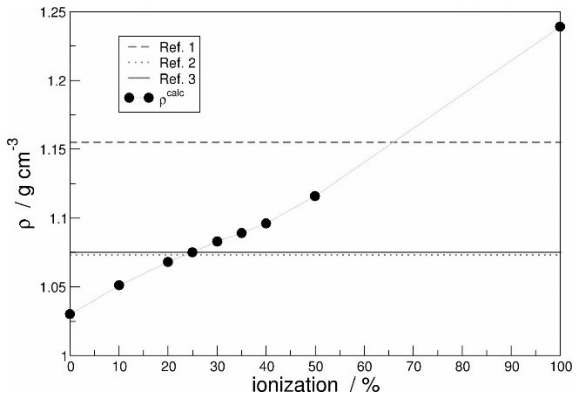

Figure 2. Calculated densities ρ^{calc} (black circles) of various compositions of ionized to non-ionized 1-methyimidazolium acetate:1-methylimidazole acetic acid solutions using polarizable MD, see Table 1, Ref. [1] (dashed grey line), Ref. [2] (dotted grey line) and Ref. [3] (solid grey line) correspond to the studies by Hou et al.[34] (1.155 g cm^{-3}), Qian et al.[35] (1.075 g cm^{-3}) and Watanabe et al.[36] (1.073 g cm^{-3}) respectively. With the light grey line providing a guide to the eye for observed points at various ionization ratios.

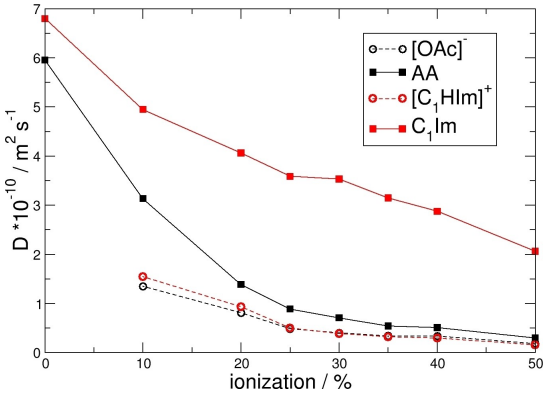

Figure 3. Diffusion coefficient of each the ions and the neutral particles at various compositions of ionized to non ionized [C_1HIm][OAc]:1-methylimidazole, acetic acid solutions calculated with the polarizable MD in a 500 ion pair + neutral molecules box.

Following this, the diffusion coefficient of the individual compounds within the system were calculated for the same systems as were used to calculate the densities at various ionization ratios. From this analysis it was found that the different molecules within the solution are able to diffuse at highly varied rates, with data shown in Figure 3.

As illustrated in this Figure, there is a large difference between the ions and the neutral molecules, with the neutral molecules diffusing at a notably faster rate than their charged counterparts. One example of this is in the 20% ionized system, wherein the 1-methylimidazole and acetic acid were shown to have diffusion coefficients of 4.06×10^{-10} m^{2}s^{-1} and 1.39×10^{-10} m^{2}s^{-1}, respectively, in comparison to 1-methyimidazolium and acetate being at 0.94×10^{-10} m^{2}s^{-1} and 0.81×10^{-10} m^{2}s^{-1} respectively. The C_1Im/[C_1HIm]$^+$ units were shown to have diffusion coefficients higher than their AA/[OAc]$^-$ counterparts as soon as the ions are part of the mixture, notably so in the case of the neutral species.

This trend is in agreement to prior experimental studies viewing the individual diffusion coefficients of [C_1HIm]$^+$ and [OAc]$^-$ in neat IL solutions.[37,38] This large difference between C_1Im and AA diffusion coefficients indicates that the hydrogen bond donating hydrogen atom on AA also hinders diffusion, likely through strong interactions with acetate anions. This is further supported by the observation that in the pure C_1Im-AA system, C_1Im and acetic acid were shown to have comparable diffusion coefficients, whereas upon the addition of [C_1HIm][OAc] the acetic acid diffusion coefficient decreased substantially faster than the C_1Im. These results agree with the previous results of Joerg and Schröder[33] wherein the ionization ratio was estimated to be between 20 and 30%. From comparing these analyses to experiment, it can be further refined to predict an ionization ratio of closer to 25% than either 20 or 30%. Therefore, for mixture calculations, the ionization ratio of 25% will be applied as a means to simulate the conditions of the neat IL at room temperature.

To assess the factors affecting the diffusion coefficients and understand the hydrogen bonds occurring, radial distribution functions (RDFs) of hydrogen bonds were analyzed. In this instance, it was shown that as the ionization percentage is increased, the acetate anion interactions as a hydrogen bond acceptor for AA and the 1-methyimidazolium cation hydrogen bond donors increases to approach a coordination number of 1, as shown below in Figure 4.

In contrast, the C_1Im hydrogen bond acceptor is shown to approach 0 as the ionization ratio increases. Interestingly, even at an ionization ratio of 10% the acetate anion acts as a stronger hydrogen bond acceptor in comparison to C_1Im, as indicated by its coordination number, despite it being at a 1:10 molar ratio. An inspection of the RDFs of each H-bond type at 25% ionization (see Figure 4 above) indicates that the acetate anion is more strongly associated as a hydrogen bond acceptor than C_1Im or the AA. The difference in magnitude indicates that less hydrogen bonds involve the C_1Im molecule in comparison to acetate anion probably due to its weaker negative charge present on the hydrogen bond acceptor center. The weaker electrostatic interactions found between C_1Im and AA may be

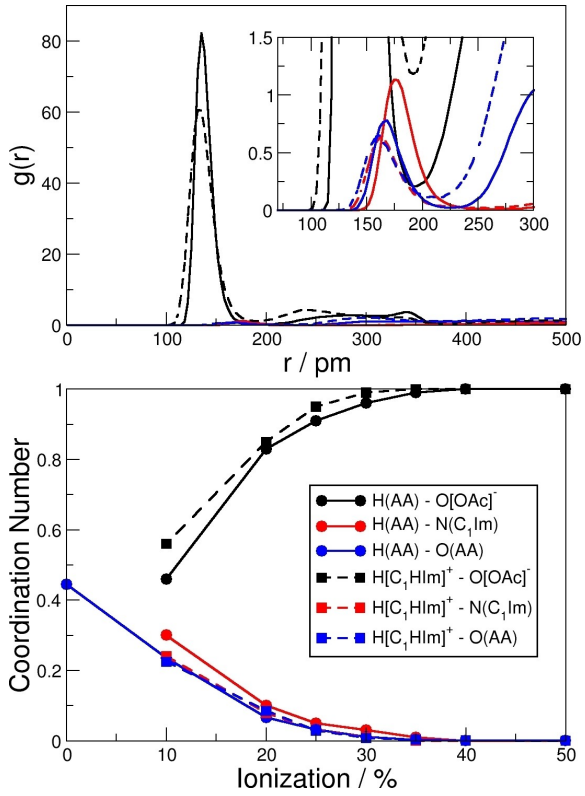

Figure 4. H–O/N structure of all species, see legend, at various ionization ratios. Above: H–O/N RDFs at 25 % ionization; Below: Integrated first peak (see Methodology section) coordination numbers.

linked to the higher diffusion coefficient previously calculated for C_1Im and 1-methylimidazolium cation units in comparison to AA and acetate anion. While the AA is involved in strong or many hydrogen bonds as a donor, it is similar weak as acceptor compared to the acetate anion, see blue curves in Figure 4.

Effect of excess acid or base

As described in the introduction, the interaction between neutral substances (in this system the base and acid molecules that are not ionized) may have a strong effect on the properties of the system. This is especially the case when one of the two components is present in excess in the solution. C_1Im and AA can, in principle, both have strong interactions with one of the ions of the salt produced by the ionization. Interactions between the AA and the acetate anion, as well as between the C_1Im and the 1-methylimidazolium cation are conceivable, potentially stabilizing the ionization products, while also disrupting the interplay between acetate and 1-methylimidazolium ions.

To observe the possible extent of these effects, we investigated the dissociation of a single [C_1Him][OAc] ion pair in AA and in C_1Im through umbrella integration. Since in classical MD simulations the transfer of charge or protons between the acetate and the acetic acid is not possible, charge delocalization is, despite the polarizable force field applied, resulting in some overbinding of the ionic species. In accordance, the separation of the ion pair to a distance of 15 Å (measured between the acidic H of the cation and the carboxyl carbon of the anion) was endothermic in both cases. However, in AA, the dissociation process was found to be significantly less energy demanding (4 kcal mol^{-1}) as in C_1Im (14 kcal mol^{-1}). For the obtained free energy profiles, see the Supporting Information.

Taking these values literally would suggest that ion pairs are more stable in solution than the separated ions. However, the trend is clear, and it can also be rationalized as a stronger interaction between the acetate and the AA than that between the C_1Im and its protonated derivative. Since an acetate anion has two oxygen atoms, each capable of interacting with one or even two AA molecules, this hypothesis seems to be fully reasonable.

It is also worth pointing out that before the full dissociation of the two oppositely charged ions, they apparently form a solvent separated ion pair in both solvents, with a H–C distance of ca. 5 Å. The trend in the relative energy of this species is also in line with the corresponding separation energy measured in the same solvent, amounting up to 0.8 kcal mol^{-1} in AA, and 5.1 kcal mol^{-1} in C_1Im.

The results described in the previous section were then compared to mixtures of a single neutral species (either C_1Im or AA) with the [C_1HIm][OAc] IL at a 25 % ionization ratio to determine the effect of addition of each neutral compound on the density and diffusion of the ion pairs, see Table 2.

When comparing the densities (Figure 5) with and without the addition of neutral molecules, the addition of C_1Im was seen to cause a linear decrease in density. This can be attributed to the calculated density of neat C_1Im having a value of 1.006 g cm^{-3} compared to the 25 % ionized sample being calculated at 1.075 g cm^{-3}. In comparison, the addition of AA had a smaller effect on the density of the system, as shown in Figure 5. Neat AA was simulated to have an average density of 1.063 g cm^{-3} and therefore making it more comparable to the 25 % ionized [C_1HIm][OAc] IL density. Due to the similar densities of AA and 25 % ionized [C_1HIm][OAc], the density is shown to vary from the linear trend observed upon the addition of C_1Im. Upon the addition of AA, there is a slight but notable

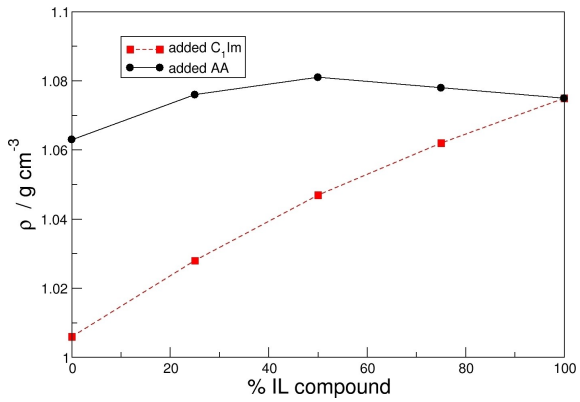

Figure 5. Density of various compositions of 25 % ionized [C1HIm][OAc]: C1Im (black) and [C1HIm][OAc]:AA (red) solutions calculated using polarizable MD in a 500 ion pair + neutral molecules box.

increase up to the point wherein AA and [C_1HIm][OAc] are at a 1:1 ratio, wherein the density is found to be 1.081 g cm^{-3}. This increase of the density of the mixture in comparison to the neat constituents therefore shows that the addition of neutral AA to the IL solution is able to increase ordering of the system, creating non-ideal mixing.

Following this, the diffusion coefficients in these systems were calculated to determine the effect of C_1Im and AA addition on the diffusion of the IL solution. In a majority of cases, the addition of neutral compounds increased the diffusion coefficient of all molecules in the system due to the higher diffusion coefficient present in neat AA of C_1Im solutions. This is in agreement with a study by Koverga et al.,[39] wherein it was found that the highest conductivity occurred at 20% IL to neutral systems, meaning increasing the IL concentration decreased the diffusion coefficient and thus conductivity. However, as shown in Figure 6, the addition of AA up to a 1:1 ratio decreases the diffusion coefficient of C_1Im from 3.59 × 10^{-10} m^2 s^{-1} for the 25% ionized neat IL to a minimum of 2.66 × 10^{-10} m^2 s^{-1}.

This indicates that while added AA allows for increased mobility for all other components, up to a 1:1 ratio with the IL, it decreases the mobility of the C_1Im. The likely reasoning for the general increase in diffusion coefficient upon addition of the neutral molecules, wherein all molecules are able to more readily diffuse is the reduction in electrostatic driven interactions. These investigations therefore indicate a complex alteration to both the density and diffusion coefficients upon the addition of AA, with both these properties showing non-linear trends upon the variation of IL:AA ratio.

In contrast, the trends upon the addition of C_1Im appear comparatively linear, indicating a unique effect of AA which C_1Im does not possess. However, in reality, it must be noted that it is possible that the neutral molecules may be able to ionize themselves within the solution, thus potentially altering the calculated densities and diffusion coefficients. As a result of the present MD simulations not allowing for alteration in topology of molecules, this possibility is not being accounted for. Therefore, it is crucial for AIMD to be applied to qualitatively determine the extent of the ionization of added C_1Im and AA.

To ascertain the impact of adding neutral C_1Im or AA to the IL mixture, RDFs of the different possible hydrogen bonds were calculated in the same manner as in the neat IL at various ionization ratios. Through this analysis, it was shown that the addition of C_1Im, and in particular AA has a substantial effect on the coordination numbers of various hydrogen bonds, as shown in Figure 7.

Specifically, it is of note that the addition of AA significantly decreases the hydrogen accepting ability of the negatively charged oxygens of acetate, such as in the case of H([C_1HIm]$^+$)-O([OAc]$^-$) hydrogen bonds, wherein the coordination number was shown to decrease from 0.95 as a neat IL to 0.40 at a 3:1 ratio of AA to IL, see Figure 7 below black curves. This suggests that AA at higher concentrations is able to disrupt the hydrogen

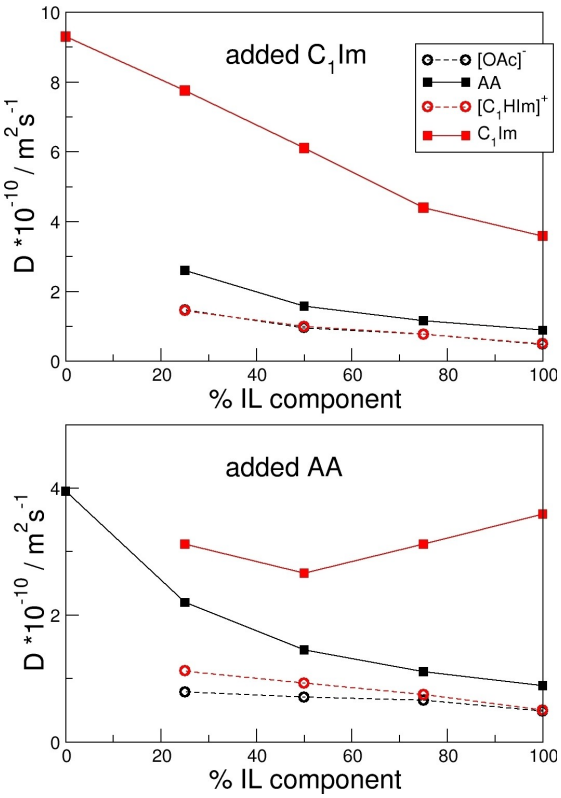

Figure 6. Diffusion coefficients of each the ions and the neutral particles at various compositions of 25% ionized [C_1HIm][OAc]:C_1Im (top) and [C_1HIm][OAc]:AA (bottom) solutions calculated using polarizable MD. Please note that the *y*-axis scale is different for top and below.

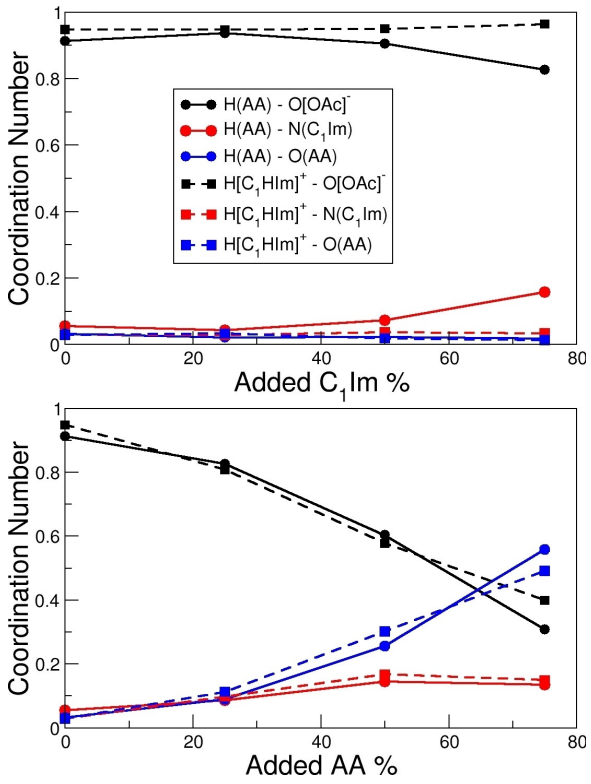

Figure 7. Coordination numbers of various compositions of 25% ionized [C1HIm][OAc]:C1Im (above) and [C1HIm][OAc]:AA (below) solutions calculated using polarizable MD.

bond accepting ability of negative oxygens on acetate, while serving as hydrogen bond acceptor for itself and the 1-methyimidazolium cation (blue curves Figure 7 below) as well as slightly increasing the hydrogen bond accepting ability of the N1 nitrogen of C_1Im with both AA and 1-methyimidazolium (red curves Figure 7 below). In addition, C_1Im was shown to play a more subtle role in the alteration of coordination numbers in hydrogen bond strength. This smaller impact on coordination numbers in comparison to the addition of AA is likely attributed to the fact that 1-methylimidazole/1-methyimidazolium has a weaker ability to donate and accept hydrogen bonding than AA/acetate as shown by the RDF $g(r)$ maximum, as shown in prior literature on the [C_1HIm][OAc] system.[26,40]

Proton transfer and ionization analysis

The AIMD analysis to determine the effect of C_1Im and AA addition to [C_1HIm][OAc] on total ionization and Grotthuss diffusion was completed with RDFs.

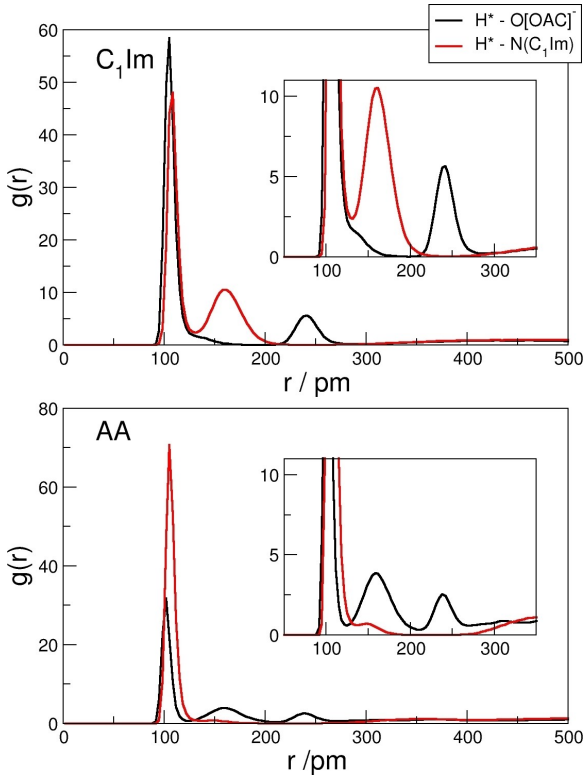

Figure 8. RDFs of [C_1HIm][OAc]:C_1Im (above) and [C_1HIm][OAc]:AA (below) at 75% added molecules.

This provided contrast to the above simulations (see Figure 7) since it allows for the making and breaking of H*-O([OAc]$^-$) and H*-N(C_1Im) bonds in AA and 1-methyimidazolium, respectively, something which is not possible in the above applied MD.

It can be clearly noted in Figure 8 that there are two (red: above and below, black: above) and three (black: below) distinct peaks in the RDFs. The first of these peaks, corresponding to covalent bonding for the proton with AA and 1-methyimidazolium was found to have a maximum at a distance of 102 and 108 pm for AA and 1-methyimidazolium, respectively, as shown in Figure 8.

However, the second peak corresponds to hydrogen bonding between the protons and the hydrogen bond acceptors with a distance of 155 and 158 pm for acetate in the [C_1HIm][OAc] mixture with AA or C_1Im added. Note, this hydrogen bond is almost absent for the AA to the actetate anion when additional C_1Im molecules and vice versa for the 1-methyimidazolium cation to the C_1Im molecule when additional AA molecules are added in the 75% added base or acid systems. In contrast to this in the earlier study on the 50:50 [C_1HIm][OAc] system,[26] i.e., the "pure" PIL, these hydrogen bonds are present for both hydrogen bond acceptors. Note, that the third/ second peak at 242 pm in the black curves (Figure 8) is due to the second oxygen atom in the acetate ion/ AA molecule.

From integrating these RDFs to the first RDF minimum (Figure 8), we can further deduce the ionization percentages at different compositions, see the 2nd and 3rd column of Table 3. In the case of 1-methyimidazolium it was taken as 66% if the number integral was 0.66 for example. Whereas in the AA case if the number integral was 0.69, then the ionization was set to (100-69)% = 31% due to in this case a coordination number of 1 meaning that all would be AA. The results show that the ionic density increases with increased $x_{[C_1HIm]^+C_1Im}$. Keeping in mind the ionic ratio of 20 to 35% obtained previously for the "pure" PIL ($x_{[C_1HIm]^+C_1Im} = 0.5$)[26] we can infer that little or no change in ionic density results upon the addition of AA to the PIL. In contrast, a large increase of ionic species occurred from the addition of C_1Im to $x_{[C_1HIm]^+C_1Im} = 0.5$ system.

Further, the coordination number with respect to the hydrogen bonding (second peak in the RDF of Figure 8) are presented in the 4th and 5th column of Table 3. The hydrogen bonding was found to be largest in the 75% added neutral molecule systems for the added molecule species or its corresponding ion, but in the 50% composition a difference between added AA and added C_1Im occurred. While 50% AA still shows large amount of hydrogen bonding for the

Table 3. Ionization (explained in text), as well as hydrogen bonding coordination numbers (NH*B*) from/to the H* hydrogen atom. $x_{[C_1HIm]^+C_1Im}$ given as *x*.

% added	% [C_1HIm]$^+$	% [OAc]$^-$	N^{HB} C_1Im	N^{HB} [OAc]$^-$	*x*
75 AA	24	23	0.0/0.1	0.9/0.5	0.2
50 AA	31	30	0.2/0.3	0.8/0.4	0.33
50 C_1Im	46	43	0.6/0.3	0.4/0.2	0.66
75 C_1Im	66	60	0.9/0.2	0.0/0.0	0.8

corresponding species, 50% C_1Im strongly dropped the amount of hydrogen bonds for the corresponding species while the hydrogen bond to the acetate anion is much more pronounced than vice versa. This implies that on the AA side more Grotthuss diffusion is possible, because next to the amphoteric nature of AA/$[OAc]^-$ which $[C_1HIm]^+$/C_1Im lacks, the prerequisite of a much more extended hydrogen bonding network was observed.

So far we did not provide data that showed how the anion and base molecules interact with each other. In order to see this we evaluated the corresponding center of mass RDFs. For each composition the overall picture is different, but the individual C_1Im-$[OAC]^-$ interaction is similar in all cases – with the exception of at high AA wherein the distance is shifted by approximately 10 pm, shown in Figure 9 . In contrast, there is shown to be large differences in the like-unit interactions. In the case of the C_1Im-C_1Im interplay, the maximum shifted at high AA composition to high C_1Im by almost 170 pm where the original peak transformed into a prepeak or shoulder. Similarly, the $[OAC]^-$-$[OAC]^-$ interaction shifted by 100 pm when going from high to low AA concentration. If one recalls the behavior of a true IL, where the counter-ions provide the closest distance and the like-ions are shifted to larger distances, it is clear that such a behavior is mostly seen in the high C_1Im composition whilst altering the composition, the compounds, especially the high AA composition behaves differently.

Following this, the trajectory was visualized to further understand the ability of these larger hydrogen bonding networks to facilitate proton transfer. In this analysis, it can be seen that the addition of AA allows for long chains comprised of primarily acetic acid/acetate compounds, but also with the potential of imidazole/imidazolium being involved. These are shown to be able to shuttle protons over the chain on a ps timescale between several molecules, in a way that if viewed on a larger scale than is available in AIMD, could allow for charges to diffuse rapidly across large distances. It is particularly notable in these systems such that the initial transfer of one proton can have downstream effects on other molecules in the chain. This is seen in Figure 10, wherein the transfer of the proton marked in dark blue originally belonging to imidazolium can facilitate the transfer of the proton in light blue, which then facilitates the proton marked in brown. This chain reaction gives insight into the mechanism by which large-scale Grotthuss diffusion may be enhanced when the "neat" 50:50 IL is doped with AA to allow these networks to be propagated.

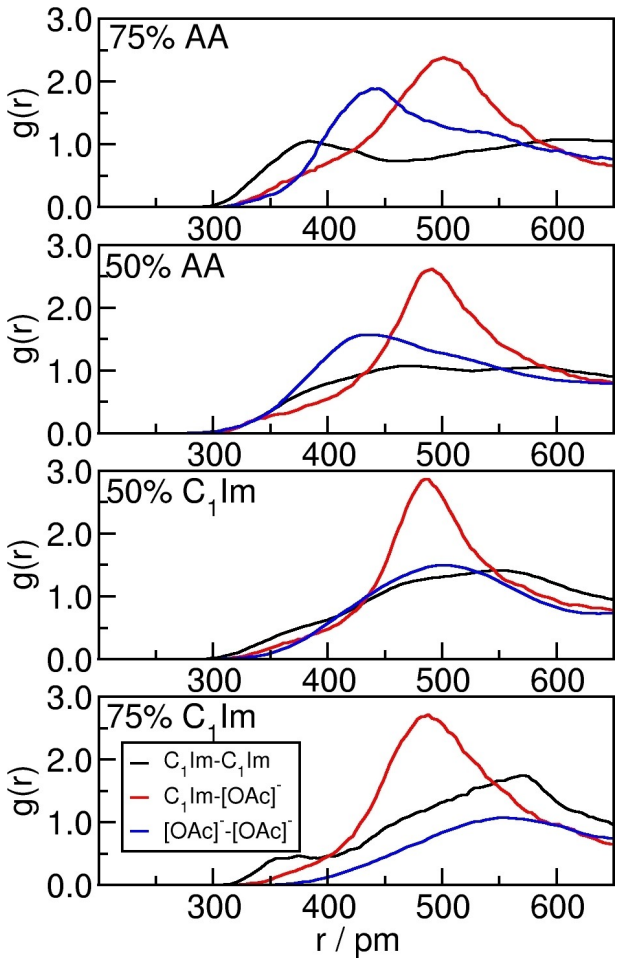

Figure 9. Center of mass (COM) RDFs of C_1Im with other C_1Im units (black) and with $[OAC]^-$ (red) as well as $[OAC]^-$ with other $[OAC]^-$ units (blue).

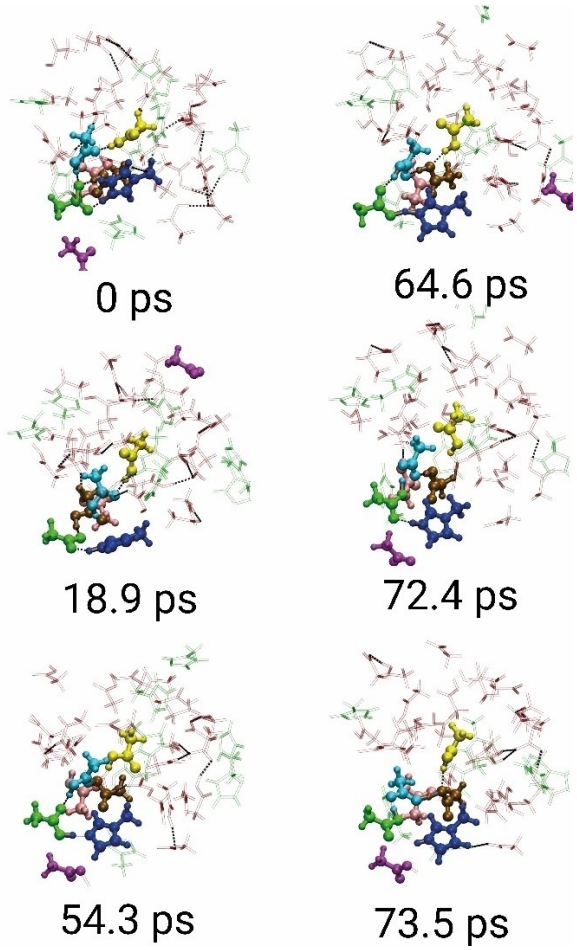

Figure 10. Visualization of the 75% AA, 25% $[C_1HIm][OAc]$ at various timesteps, with the notable hydrogen bonding network highlighted throughout.

Conductivity along the mole fraction range

To observe how the effects described above precipitate into conductivity when varying the C_1Im/AA molar ratio, we performed conductivity measurements over the full concentration range. When ionizing C_1Im with adding AA to it gradually, a steady increase in conductivity is observed, as indicated by Figure 11.

Although one might expect that the 1:1 ratio, i.e. x should produce the most ions, and thereby the highest conductivity, the results exhibit further increase in the conductivity beyond this point upon the addition of more AA (with even slightly less ionization), until the ratio of 2:1, i.e., $x_{[C_1HIm]^+C_1Im} = 0.33$. At this concentration, the conductivity reaches a plateau, with a slower, but further increase until ca. $x_{[C_1HIm]^+C_1Im} = 0.12$. Increasing the concentrations of AA further results in a sudden drop of the conductivity, presumably due to the decrease in the ion density of the solution.

As discussed in the introduction, it is in principle possible to explain changes in the conductivity through changes in viscosity. Thus, the question can be raised, if the higher conductivity of AA-rich solutions (from $x_{[C_1HIm]^+C_1Im} = 0.5$ to 0.2) can be explained by diluting the ionic compound with a molecular solvent, which makes the solution more fluid and more conducting. However, the computational diffusion coefficients of the ions do not seem to indicate that the ion mobility is responsible for this effect or at least not to a significant extent. Furthermore, if the high conductivity at the AA-rich range would occur due to a mere dilution process, similar effects should be observed in the C_1Im-rich concentration range as well, especially since the latter compound has the lower viscosity of the two as a pure substance.

As seen from the umbrella integration calculations, higher AA concentrations seem to improve the dissociation of ion pairs into individual ions through the strong interactions between the acid and the acetate. Due to the dissociation, the ion movements are more independent, and thus can contribute to the charge transport more efficiently, which increases the conductivity. The onset of the plateau, at $x_{[C_1HIm]^+C_1Im} = 0.3$ (corresponding to an acid/base ratio of 2:1) seems to support the idea of a single AA being ionized, while the thereby formed acetate being solvated by another acid. At a slightly larger AA/Im ratio, at $x_{[C_1HIm]^+C_1Im} = 0.25$, more AA molecules are available, which must leave – even with a hypothetical full dissociation – two acid molecules unreacted, available for the solvation of the acetate.

However, at $x_{[C_1HIm]^+C_1Im} = 0.12$, after complete ionization seven AA molecules would remain in the solution. Since a single acetate anion does not accept seven hydrogen bonds through its oxygen atoms, but rather one to four (see data above), the acid molecules above that number should not be able to contribute to separating the 1-methylimidazolium acetate ion pair. Instead, these extra acids should simply decrease the concentration of the ionic species, which would then decrease the overall conductivity. On the other hand, the high concentration of AA allows for the formation of an extensive hydrogen bonding network, which stretches through the mixture and is a pre-requisite for Grotthuss diffusion. Thus, the width of the plateau can be best explained through Grotthuss diffusion. Considering that the plateau is apparently the result of two effects that increase conductivity, it is noteworthy that it slightly resembles a double peak. Although the minimum between the peaks is so shallow that one might speculate that it may also be a result of the uncertainties of the measurements, it was found to be reproducible in the experiments.

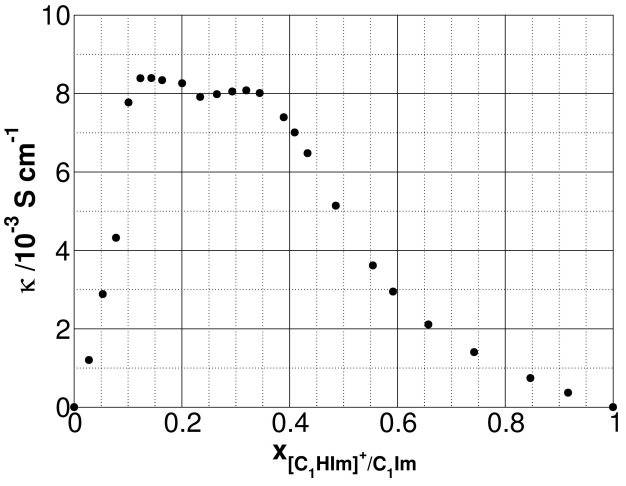

Figure 11. Conductivity plotted against the mole fraction of C_1Im, which results in $x_{[C_1HIm]^+C_1Im}$, see Table 2.

Correlation between theory and experiment

When comparing the results obtained from theory to the conductivity obtained experimentally, it is important to assess the various physical properties calculated and determine their role in the conductivities observed. The analysis of diffusion coefficients obtained upon the variation of ionization determined that the more ionic particles are in the system the slower the diffusion, see Figure 3. This partially correlates to the conductivities viewed experimentally, wherein at $x = 0.5$ we expect the "pure PIL" and hence the highest ionic density. While it is possible that ions are able to move together in this instance, data from umbrella integration suggest ions are favored to dissociate. This thus correlates to observations that diffusion is somewhat inversely proportional to ionization in solutions, thus lowering the conductivity of the 50% AA, 50% C_1Im system.

Following this, neutral molecules were added neutral to a fixed ionic density of 25% determined to align with experiment. The density of the system upon the alternation of the ratio of AA to C_1Im is shown to be proportional to the conductivity of the system. In this case, the system composition wherein density is at a maximum is consistent with the ratio wherein conductivity is shown to be at a maximum and then it drops, see Figure 5. In the case of analyzing the relationship between the diffusion coefficient and conductivity upon addition of neutral molecules, there is no obvious correlation. In this case, as shown in Figure 6, theoretically the addition of either

molecule is shown to increase the diffusion coefficient. However, in experiment only AA addition increases the conductivity, whilst C_1Im addition is seen to cause decrease. Therefore, while a notable rate of diffusion may be beneficial to improving conductivity, it is not solely responsible for the amount of observed conductivity in this system. When analyzing the interaction between separate molecules, Figure 7 details how specific interactions can prove vital in understanding conductivity trends. Specifically, the trends noted here underpins the importance of specific hydrogen bonding networks facilitating high conductivity. This analysis showed, in the system closest to maximum observed conductivity (25% to 75% added acetic acid (AA)) the AA-AA hydrogen bond coordination number are relatively equivalent to with the coordination number of AA-Anion hydrogen bonds. From this equilibrium, increasing the IL concentration was seen to decrease the AA-AA hydrogen bonds, breaking potential hydrogen bonding networks. Conversely, on the C_1Im side, upon addition of C_1Im there is no similar neutral-ionic interactions, with only a very strong hydrogen bond between cation-anion noted. This therefore leads one to believe that extensive hydrogen bonding networks are capable of forming in acetic acid heavy systems which are unavailable in those with excess 1-methylimidazolium, as depicted in Figure 12. Therefore, in future systems utilizing Grotthuss transfer, it is necessary to strike a balance between a system wherein proton transfer can happen to a sufficient degree, but also those which are capable of forming extended hydrogen bonding networks.

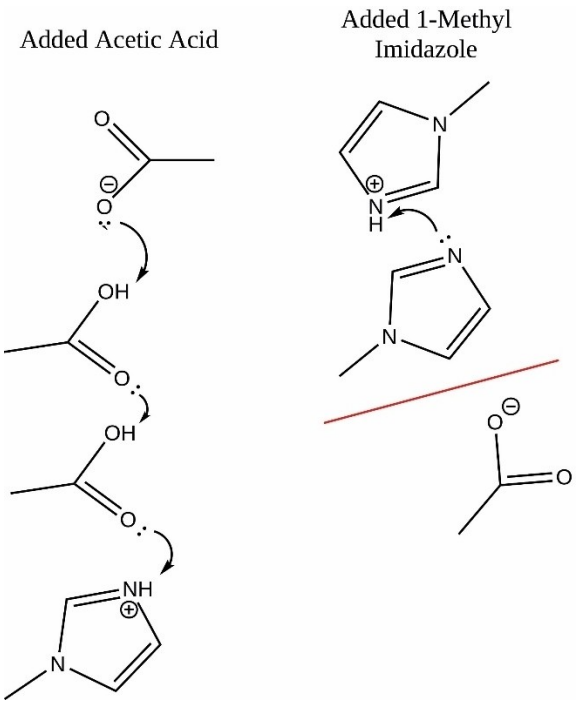

Figure 12. Mechanism for potential Grotthuss diffusion in systems of $[C_1HIm][OAc]$ with added acetic acid (left) and 1-methylimidazole (right)

Conclusions

Overall, it can be seen that the factors influencing the conductivity in asymmetrical pseudo-protic ionic liquids are varied and vast. Ionization of the IL, as well as the addition of acetic acid and 1-methylimidazole were found to dramatically effect conductivity through their effects on density, diffusion and perhaps most importantly of all, hydrogen bond network formation. Specifically, the addition of acetic acid to the neat IL caused an increase in conductivity, seen to be in line with an observed non-linear change in density. In this case, a 1:1 mixture of acetic acid to 25% ionized IL was found to have a higher density than either neat sample. This indicates that the change in interactions through increased hydrogen bonding interactions can facilitate tighter packing of the molecules. In addition to this, the analysis of RDFs highlighted the importance of creating hydrogen bond networks between AA and $[OAc]^-$ molecules in facilitating long range proton shuttling. In this case, adding AA to the system was shown to yield high AA-AA coordination numbers as well as maintaining strong AA-$[OAc]^-$ interactions. This system was observed to produce the highest conductivity experimentally and thus correlates theoretical hydrogen bonding with experimental conductivity.

Through analysis of AIMD, it is further seen that addition of acetic acid and 1-methylimidazole had inverse effects on ionization, as well as hydrogen bonding chain distributions. Acetic acid was shown to form strong, stabilizing hydrogen bonding networks between neighboring acetic acid and acetates which were found to improve the ability for long-range proton shuttling. In contrast, the addition of 1-methylimidazole increased proton transfer between neighboring acetic acid and 1-methylimidazole molecules on a picosecond timescale, but did not form networks necessary for Grotthuss diffusion. Therefore, it can be concluded that the longer hydrogen bonding chains observed in acetic acid heavy systems may be favorable for Grotthuss diffusion in comparison to the short chains found with added 1-methylimidazole, that are only capable of proton hopping.

Therefore, these results provide theoretical insight to the impact of neutral molecule addition on physical properties and structure which may potentially affect Grotthuss diffusion in phenomena examined experimentally by Smith *et al.*[27] However, in contrast to Smith *et al.*, the neutral molecule being added was in some cases found to induce a decrease of conductivity. This was determined to be related to several factors, namely ability to form hydrogen bond networks, diffusion, ionization and proton transfer ability, providing a theoretical link between the ability of large hydrogen bonding complex formation and conductivity in these fascinating pseudo-protic IL systems. The above described, more fundamental structural picture can be used to design more intricate electrolyte mixtures to suit specific electrochemical applications, offering further tunability to the already diverse array of pseudo-protic IL electrolytes.

Experimental Section

Polarizable MD simulations

To obtain accurate structural and transport properties, large-scale polarizable MD was applied with the LAMMPS software package. CL&Pol parameters were used for the ionized molecules $[C_1HIm]^+$ and $[OAc]^-$.[41,42] In the cases of the neutral molecules, acetic acid and 1-methylimidazole, OPLS-AA parameters were chosen for the Lennard-Jones non-bonding parameters as well as classical MD bonding parameters. Scaling of LJ parameters to account for explicit polarization was completed by optimizations using the B97-D3 functional[43] with a cc-pVDZ basis set[44] to obtain dimer lengths, as outlined in prior studies on IL systems. Atomic charges as well as dipoles for neutral molecules for non-bonding parameters and Drude particle addition were calculated using the CHELPG charge method[45] and the MP2/cc-pVTZ level of theory on structures optimized as outlined for bonding parameters. Neat IL simulations were then constructed using 500 total pairs of 1-methylimidazole/1-ethyimidazolium and acetate/acetic acid with the PACKMOL software program.[46] These systems were then equilibrated for 2 ns at 300 K employing a Nosé-Hoover chain thermostat[47] in an NpT ensemble with 1 fs timesteps. A production run was then commenced in an NVT ensemble for 5 ns with the same temperature and thermostat as in the equilibration. From the production run, physical properties such as density and diffusion coefficient were calculated employing the TRAVIS software package.[48,49] Parameters were validated by comparing the resulting diffusion coefficients of neat 1-methylimidazole and acetic acid to values obtained in prior studies with the aid of experiment and AIMD calculations.[50,51] Both diffusion coefficients found in this study to fall within the same magnitude as those prior and thus ensuring the validity of transport calculated. The diffusion coefficients were used to estimate the ideal conductivity using the Nernst-Einstein equation. Radical distribution functions (RDFs) were calculated for the interactions between hydrogen bond donors 1-methyimidazolium and acetic acid with the hydrogen bond acceptor of 1-methylimidazole and acetate. The reference molecules constituted of the hydrogen attached to the N1, as labelled in 1 of 1-methyimidazolium and the hydrogen of the carboxylic acid group of acetic acid, while the N1 of 1-methylimidazole and the two oxygens of carboxylate group of acetate were used as the observed molecules. Coordination numbers were obtained by taking the integral of all points up until the first minima, which is defined as the end of the first solvation shell. The first minima is described as being a point which is surrounded by more positive values in the range of 0.2 Å both in the positive and negative direction. Densities were compared to literature values found experimentally, namely, 1.155 g cm^{-3},[34] 1.075 g cm^{-3}[35] and 1.073 g cm^{-3}.[36]

AIMD simulations

Initial boxes for analysis with ab initio molecular dynamics (AIMD) were set up with the total system size of ion pairs plus neutral molecules being at 32, with ratios of both 50:50 ion pairs to neutral molecules and 25:75 ion pairs to neutral molecules tested, with both 1-methylimidazole and acetic acid tested as the neutral molecules. For example, in the 50:50 sample with 1-methylimidazole added, the system was setup to contain 16 $[C_1Him]^+$ cation, 16 [OAc] anions and 16 1-methylimidazole neutral molecules, with all system compositions shown in Table 1 These systems were placed into a box size at the density calculated through polarizable MD for the 500 molecule systems These systems were then equilibrated using an NpT ensemble with polarizable MD for 2 ns at 300 K. AIMD was then performed on the system equilibrated by classical MD using CP2 K software package with the build-in QUICKSTEP module.[52] The revPBE functional was chosen with D3 dispersion correction as the method to both optimize the structure and calculate the trajectory due to its previously established ability to simulate liquid phase systems in AIMD.[53–55] The double-ζ molecularly optimized basis set (DZVP-MOLOPT-SR-GTH)[56] basis set was utilized for all atoms with the Goedecker-Teter-Hutter (GTH) pseudopotentials chosen for core electrons with the number of valence electrons given as follows: H(1), C(4), N(5), O(6). Initially an optimization was performed with the CG optimizer and a Ry density CUTOFF criterion of 280 and Nosé-Hoover massive thermostating, with an SCF convergence criterion of 10^{-5}. Timesteps of 0.5 fs are used for both equilibration and the production runs with 10000 steps equating to a duration of 5 ps employed for equilibration and 200000 steps equating to 100 ps for production. In the production run the Ry density CUTOFF criterion was increased to 400 with an SCF convergence criterion of 10^{-6}. The temperature was set to 320 K for all systems. All input files are available upon request. Analysis of AIMD was completed in a similar manner to polarizable MD with the software package TRAVIS.[48,49] RDFs were calculating using the same groups as in the polarizable MD, with the hydrogen now no longer explicitly bound to acetic acid or 1-methyimidazolium. Thus as a result, all initial bonds between labile hydrogens and 1-methyimidazolium nitrogens or acetic acid oxygens are manually broken in TRAVIS during molecule recognition so that hydrogens can be treated separately in analysis. When determining the coordination number for covalent bonds and hydrogen bonds, these are differentiated by the solvation shell number, with covalent bonds occupying the first solvation shell, whilst hydrogen occupy the second. Therefore, covalent bonds are calculated in the same manner as the coordination numbers are calculated by in polarizable MD simulations. However, the hydrogen bonding coordination number is calculated as the integral of the $g(r)$ at distances between the first and second minima.

Umbrella integration simulations

To investigate the dissociation of the 1-methylimidazolium acetate ion pair in acetic acid and in 1-methylimidazole, umbrella integration simulations were performed. In these simulations, the same polarizable force field as used in earlier classical MD calculations based on the CL&Pol and OPLS-AA force fields was applied.[41,57] Two boxes were created with a single ion pair and 200 acetic acid or 150 1-methylimidazole. After 2 ns of initial equilibration in the NpT ensemble (300 K, 1 bar), an external harmonic potential was defined between the carboxylate carbon atom of the acetate and the NH hydrogen atom of the cation with a minimum at a distance of 2 Å. The system was equilibrated in an NVT ensemble (300 K) for 500 ps, and simulated for a further 250 ps, during which the forces affected through the external potential were averaged. The NVT equilibration and production runs were then repeated, while moving the minimum of the external potential with 0.25 Å increments up to 15 Å. Integrating the average forces obtained at each distance against the distance gave the free energy function discussed in the article.

Conductometry measurements

Conductivity of acetic acid-1-methylimidazole mixtures was measured by a Consort C3010 multi-parameter analyzer connected to a Radelkis OK-9023 bell electrode. The calibration of the electrode was carried out for 0.01 M and 0.1 M KCl (Spektrum-3D) solutions (1.412 and 12.88 mS cm^{-1}, respectively) at 25 °C. Due to the potential sensitivity of the conductivity to moisture, special efforts were made to exclude water from the samples. 1-Methylimidazole ($\geq$ 99 %, purified by redistillation, $<$ 0.005 % water, Merck KGaA, in

Sure/Seal) and glacial acetic acid (≥99.8%, AnalaR NORMA PUR ACS, Reag. Ph. Eur., ≤0.25% water, VWR International Ltd) were used as-received without any further purification. All manipulations were carried out using Schlenk techniques under an atmosphere of argon (Argon 4.6; ≥99.996% Ar). The purity of 1-methylimidazole was verified by ^{1}H NMR spectroscopy (360 MHz Bruker Avance I. NMR instrument, equipped with a 5 mm direct QNP probe head, T=298 K), which exhibited no signal that could be assigned to water. Upon adding 2.5 w/w% water to the material, a distinct peak at 4.7 ppm was observed, see the Supporting Information.

Author Contributions

The manuscript was written through contributions of all authors. All authors have given approval to the final version of the manuscript.

Acknowledgements

M.K. is grateful for the National Research, Development and Innovation Office of Hungary (OTKA-PD 135169) for financial support. The financial support for O.H. by the National Research, Development and Innovation Office through the project OTKA-FK 138823 is gratefully acknowledged. Furthermore, O.H. is grateful for the support from the János Bolyai Research Scholarship of the Hungarian Academy of Sciences, and the ÚNKP-22-5 New National Excellence Program from the National Research, Development and Innovation Fund. A.U. was supported through the National Research, Development and Innovation Office through the project RRF-2.3.1-21-2022-00009, entitled National Laboratory for Renewable Energy, implemented with the support provided by the Recovery and Resilience Facility of the European Union within the framework of the Programme Széchenyi Plan Plus. Open Access funding enabled and organized by Projekt DEAL.

Conflict of Interests

The authors declare no conflict of interest.

Data Availability Statement

The data that support the findings of this study are available from the corresponding author upon reasonable request.

Keywords: binary electrolytes · autocorrelation functions · Grotthuss diffusion · ionic liquids · polarizable molecular dynamics

[1] J. J. Kosinski, P. Wang, R. D. Springer, A. Anderko, *Fluid Phase Equilib.* **2007**, *256*, 34.
[2] A. Persat, M. E. Suss, J. G. Santiago, *Lab Chip* **2009**, *9*, 2454.
[3] C. Malm, L. A. Prädel, B. A. Marekha, M. Grechko, J. Hunger, *J. Phys. Chem. B* **2020**, *124*, 7229.
[4] P. Y. Nakasu, C. J. Clarke, S. C. Rabelo, A. C. Costa, A. Brandt-Talbot, J. P. Hallett, *ACS Sustainable Chem. Eng.* **2020**, *8*, 7952.
[5] H. Doi, X. Song, B. Minofar, R. Kanzaki, T. Takamuku, Y. Umebayashi, *Chem. Eur. J.* **2013**, *19*, 11522.
[6] H. Watanabe, T. Umecky, N. Arai, A. Nazet, T. Takamuku, K. R. Harris, Y. Kameda, R. Buchner, Y. Umebayashi, *J. Phys. Chem. B* **2019**, *123*, 6244.
[7] L. Konermann, S. Kim, *J. Chem. Theory Comput.* **2022**, *18*, 3781.
[8] S. Kang, A. Singh, K. G. Reeves, J.-C. Badot, S. Durand-Vidal, C. Legein, M. Body, O. Dubrunfaut, O. J. Borkiewicz, B. Tremblay, C. Laberty-Robert, D. Dambournet, *Chem. Mater.* **2020**, *32*, 9458.
[9] R. Kanzaki, K. Uchida, X. Song, Y. Umebayashi, S.-i. Ishiguro, *Anal. Sci.* **2008**, *24*, 1347.
[10] D. Shang, X. Zhang, S. Zeng, K. Jiang, H. Gao, H. Dong, Q. Yang, S. Zhang, *Green Chem.* **2017**, *19*, 937.
[11] T. L. Greaves, C. J. Drummond, *Chem. Rev.* **2015**, *115*, 11379.
[12] T. Vogl, S. Menne, R.-S. Kühnel, A. Balducci, *J. Mater. Chem.* **2014**, *2*, 8258.
[13] G. Huang, L. Porcarelli, M. Forsyth, H. Zhu, *J. Phys. Chem. Lett.* **2021**, *12*, 5552.
[14] J. A. Widegren, J. W. Magee, *J. Chem. Eng. Data* **2007**, *52*, 2331.
[15] Y. Kohno, H. Ohno, *Chem. Commun.* **2012**, *48*, 7119.
[16] K. Ueno, H. Tokuda, M. Watanabe, *Phys. Chem. Chem. Phys.* **2010**, *12*, 1649.
[17] H. Tokuda, S. Tsuzuki, M. A. B. H. Susan, K. Hayamizu, M. Watanabe, *J. Phys. Chem. B* **2006**, *110*, 19593.
[18] B. Kirchner, F. Malberg, D. S. Firaha, O. Hollóczki, *J. Phys. Condens. Matter* **2015**, *27*, 463002.
[19] O. Hollóczki, F. Malberg, T. Welton, B. Kirchner, *Phys. Chem. Chem. Phys.* **2014**, *16*, 16880.
[20] P. Choi, N. H. Jalani, R. Datta, *J. Electrochem. Soc.* **2005**, *152*, E123.
[21] B. Kirchner, A. P. Seitsonen, *Inorg. Chem.* **2007**, *46*, 2751.
[22] V. K. Thorsmølle, G. Rothenberger, D. Topgaard, J. C. Brauer, D.-B. Kuang, S. M. Zakeeruddin, B. Lindman, M. Grätzel, J.-E. Moser, *ChemPhysChem* **2011**, *12*, 145.
[23] O. Hollóczki, *ACS Sustainable Chem. Eng.* **2018**, *7*, 2626.
[24] O. Hollóczki, A. Wolff, J. Pallmann, R. E. Whiteside, J. Hartley, M. A. Grasser, P. Nockemann, E. Brunner, T. Doert, M. Ruck, *Chem. Eur. J.* **2018**, *24*, 16323.
[25] A. A. Moses, C. Arntsen, *Phys. Chem. Chem. Phys.* **2023**, *25*, 2142.
[26] J. Ingenmey, S. Gehrke, B. Kirchner, *ChemSusChem* **2018**, *11*, 1900.
[27] D. E. Smith, D. A. Walsh, *Adv. Energy Mater.* **2019**, *9*, 1900744.
[28] A. Jarosik, S. R. Krajewski, A. Lewandowski, P. Radzimski, *J. Mol. Liq.* **2006**, *123*, 43.
[29] J.-F. Wang, C.-X. Li, Z.-H. Wang, Z.-J. Li, Y.-B. Jiang, *Fluid Phase Equilib.* **2007**, *255*, 186.
[30] T. L. Greaves, D. F. Kennedy, S. T. Mudie, C. J. Drummond, *J. Phys. Chem. B* **2010**, *114*, 10022.
[31] H. Watanabe, N. Arai, Y. Kameda, R. Buchner, Y. Umebayashi, *J. Phys. Chem. B* **2020**, *124*, 11157.
[32] J. Blasius, J. Ingenmey, E. Perlt, M. von Domaros, O. Hollóczki, B. Kirchner, *Angew. Chem. Int. Ed.* **2019**, *58*, 3212.
[33] F. Joerg, C. Schröder, *Phys. Chem. Chem. Phys.* **2022**, *24*, 15245.
[34] H.-Y. Hou, Y.-R. Huang, S.-Z. Wang, B.-F. Bai, *Acta Phys. -Chim. Sin.* **2011**, *27*, 2512.
[35] W. Qian, Y. Xu, H. Zhu, C. Yu, *J. Chem. Thermodyn.* **2012**, *49*, 87.
[36] H. Tokuda, K. Hayamizu, K. Ishii, M. A. B. H. Susan, M. Watanabe, *J. Phys. Chem. B* **2005**, *109*, 6103.
[37] C. A. Hall, K. A. Le, C. Rudaz, A. Radhi, C. S. Lovell, R. A. Damion, T. Budtova, M. E. Ries, *J. Phys. Chem. B* **2012**, *116*, 12810.
[38] A. Radhi, K. A. Le, M. E. Ries, T. Budtova, *J. Phys. Chem. B* **2015**, *119*, 1633.
[39] V. A. Koverga, Y. Smortsova, F. A. Miannay, O. N. Kalugin, T. Takamuku, P. Jedlovszky, B. Marekha, M. N. D. Cordeiro, A. Idrissi, *J. Phys. Chem. B* **2019**, *123*, 6065.
[40] R. Jacobi, F. Joerg, O. Steinhauser, C. Schröder, *Phys. Chem. Chem. Phys.* **2022**, *24*, 9277.
[41] K. Goloviznina, J. N. Canongia Lopes, M. Costa Gomes, A. A. Pádua, *J. Chem. Theory Comput.* **2019**, *15*, 5858.
[42] K. Goloviznina, Z. Gong, A. A. Padua, *Wiley Interdiscip. Rev.: Comput. Mol. Sci.* **2022**, *12*, e1572.
[43] L. Goerigk, S. Grimme, *Phys. Chem. Chem. Phys.* **2011**, *13*, 6670.
[44] T. H. Dunning Jr, *J. Chem. Phys.* **1989**, *90*, 1007.
[45] C. M. Breneman, K. B. Wiberg, *J. Comput. Chem.* **1990**, *11*, 361.
[46] L. Martínez, R. Andrade, E. G. Birgin, J. M. Martínez, *J. Comput. Chem.* **2009**, *30*, 2157.

[47] D. J. Evans, B. L. Holian, *J. Chem. Phys.* **1985**, *83*, 4069.
[48] M. Brehm, B. Kirchner, *J. Chem. Inf. Model.* **2011**, *51*, 2007.
[49] M. Brehm, M. Thomas, S. Gehrke, B. Kirchner, *J. Chem. Phys.* **2020**, *152*, 164105.
[50] V. Vitagliano, P. Lyons, *J. Am. Chem. Soc.* **1956**, *78*, 4538.
[51] Z. Long, A. O. Atsango, J. A. Napoli, T. E. Markland, M. E. Tuckerman, *J. Phys. Chem. Lett.* **2020**, *11*, 6156.
[52] J. VandeVondele, M. Krack, F. Mohamed, M. Parrinello, T. Chassaing, J. Hutter, *Comp. Phys. Commun.* **2005**, *167*, 103.
[53] L. R. Pestana, N. Mardirossian, M. Head-Gordon, T. Head-Gordon, *Chem. Sci.* **2017**, *8*, 3554.
[54] A. Bankura, A. Karmakar, V. Carnevale, A. Chandra, M. L. Klein, *J. Phys. Chem. C* **2014**, *118*, 29401.
[55] I.-C. Lin, A. P. Seitsonen, I. Tavernelli, U. Rothlisberger, *J. Chem. Theory Comput.* **2012**, *8*, 3902.
[56] J. VandeVondele, J. Hutter, *J. Chem. Phys.* **2007**, *127*, 114105.
[57] W. L. Jorgensen, D. S. Maxwell, J. Tirado-Rives, *J. Am. Chem. Soc.* **1996**, *118*, 11225.

Manuscript received: April 15, 2023
Revised manuscript received: June 25, 2023
Accepted manuscript online: June 26, 2023
Version of record online: ■■, ■■

RESEARCH ARTICLE

The pseudo-protic ionic liquid [C_1Hlm][OAc] was investigated with additional 1-methylimidazole and acetic acid to determine effects on conductivity and their causes. It was found that additional acetic acid increased conductivity by facilitating Grotthuss diffusion while 1-methylimidazole distrupted Grotthuss diffusion and reduced conductivity.

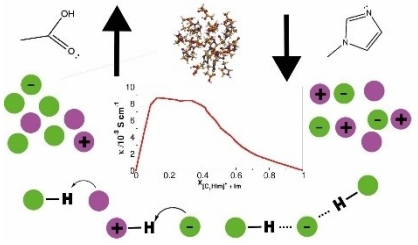

*Dr. L. Wylie, Dr. M. Kéri, Dr. A. Udvardy, Prof. Dr. O. Hollóczki, Prof. Dr. B. Kirchner**